UNIVERSITY OF CAMBRIDGE
Department of Engineering

The Effect of Bottom Stabilisation on Sheet Pile Pit

Author Name: Yan Zhuang
Supervisor: Dr Stuart Haigh

Date: May 25, 2017

I hereby declare that, except where specifically indicated, the work submitted herein is my own original work.

Signed: ____________________________ Date: ______________

Summary

Acknowledgements

Contents

1 Introduction

The world is increasingly an urban environment, and urban areas were never as crowded as they are today. In 2008, more than 50% of the world populations live in cities. By 2050 this proportion will become 70% and the urban population will be more than doubled compared to the turn of the century (Wout Broere,2015). The effective use of underground space is becoming an increasingly attractive and economical option for crowded cities. The demand of constructing reliable and durable underground space efficiently will become higher and higher in urban areas. Fig 1 shows an example of using underground space as a car park.

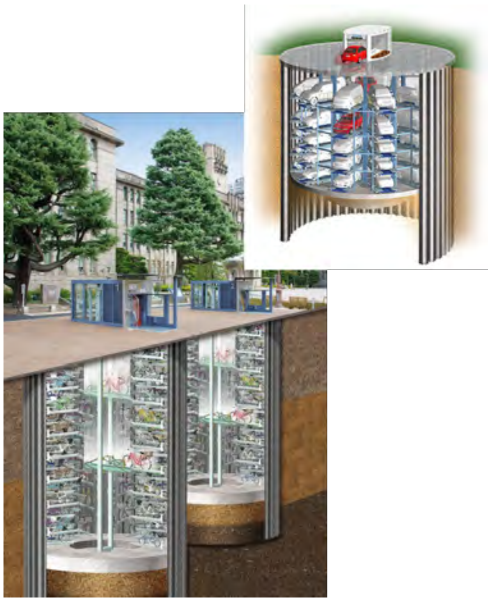

Figure 1: Giken underground parking

1.1 Sheet pile pit construction

Figure 2: Sheet pile installation by GRBS

Under ground car parks shown in Fig 1 are usually built using tubular piles or sheet piles. Tubular piles are definitely stronger but are also more expensive, if sheet piles can be used efficiently more economical underground space design can be achieved. Sheet piles are commonly used in creating underground space because of their light-weighted, recyclable and long service life properties. The traditional method of installing sheet pile walls is vibrating method, which may cause ground movement and result in settlement of adjacent structures especially in urban areas. The traditional mathod will also cause large noise that should be better avoid in the cities. The Japanese company Giken Ltd. developed the technology called GRBS (Giken Reaction Base System) to jack the pile instead of using traditional vibrating method. GRBS method utilise the uplift resistance of previously installed pile to provide reaction force required to push the new pile in by hydraulic jack. Because of the use of hydraulics, GRBS is virtually silent and vibration free with a smaller impact on surrounding soil than traditional driving procedure (Rockhill et al., 2003). Underground space can be created by jacking the piles in and form a closed area after which excavation can be done. Props will be installed during the excavation to support the sheet pile wall, which may limit the space for excavation if too many props are used. In extreme case, situation in Fig 3. may occur and it is the problem to be solved.

Figure 3: Crowded props

1.2 Ground improvement

In order to maximise the underground space, sheet piles needs to be driven into great depth to provide adequate lateral resistance, which is not always achievable in some soil conditions. The idea of bottom stabilisation or base grouting is introduced to improve the lateral resistance of soil on passive side of the piles to allow minimum amount of embedment required, so that larger underground space can be achieved under the same soil conditions. Apart from this, smaller number of props can be used during excavation to make the whole process more efficient and economical. The stabilisation prcess can be done after the installation of the piles by injecting grouts into aimed depth after which normal excavation process will be done. Usually in the underground space construction, concrete slab will be casted to form the base of the structure. This concrete slab may be replaced by the grouts injected, if the stabilisation is designed properly and this will be a much efficient construction process. However, effectiveness of the ground stabilisation is still not clear and investigations on its effect to sheet pile pit during different construction and service stages are required.

Qualitatively, injecting materials into ground will causing soil in that depth expand and apply extra horizontal stress on the sheet pile, which is equivalent to increase passive resisting stress, so that the pit will be more stable during excavation and service periods. However, the injection will also cause the pile to deflect and induce extra bending moment and shear force in the wall which may deform and damage the piles. Coming up with an appropriate design suggestion to achieve the balance between these two effects proves to be challenge because no previous design manual or researches have suggested any recommendation on this stabilisation process.

The problem is indeed complex in the following aspects. Firstly, the effect of stabilisation on soil properties is not clear, so it is impossible to link the soil property changes to the amount of grout injected directly, which means direct calculations on the pit behaviour after stabilisation can not be done. Field tests are required to obtain data of the behaviour of sheet pile pit after stabilisation, and comparisons in between different pits may be required in order to assess the effect. Secondly, even if the change in soil properties is known, simple 2D retaining wall analysis may not be adequate in this case, because the 3D behaviour of the pit may be significant. It will be difficult to obtain enough data to address the 3D behaviour of the pit because too much sensors may be required and the data collection will become a problem. In order to solve these problems, this project by taking advantages of designed field tests as well as numerical modelling will analyse the stabilisation effect qualitatively and quantitatively to give design suggestions on designs of sheet pile pit with stabilisation. Thus an assessment on the behaviour of a stabilised sheet pile pit including deflection and bending moment distribution will be made and the results can be used to calibrate the numerical modelling, which will then be used to analyse the effectiveness of the stabilisation in order to come up with a design recommendation for future constructions.

1.3 Project Aims & Challenges

This project aims to do the following:

1. Collect data from full scaled sheet pile pit field tests.

2. Analyse the data to assess the structural behaviour of the pit with and without bottom stabilisation.

3. Use Finite Element Modelling to model the pits and assess the effect of bottom stabilisation.

4. Come up with preliminary design suggestions on sheet pile pit.

Complex situations on site may affect the reliability of the data obtained, careful considerations of these factors are required in order to do sensible analysis. Correct FE analysis requires correct properties input of material and careful definition of boundary conditions, which is challenging and requires justification. Only prelimininary design suggestions will be provided, more detailed suggestions require more field tests and further investigation into the problem.

2 Literature Review

2.1 Press-in piling

Conventionally prefabricated piles are driven into ground by vibrating, which cause disruption and generate noise (David et al. 2002). Press-in piling offers an alternative way of installing piles with minimal noise and vibration. The technology is developed by Giken Ltd. and the machine they produced is called 'Silent Piler'. The silent piler grasps previously installed piles and derives reaction force from the negative skin friction and interlock resistance of these reaction piles. This reaction force provides press-in force to hydraulically jack the subsequent piles into ground (Giken Construction Revolution Vol.1, 2001). The mechanism is shown in Fig 4. 'Silent Piler' makes the most use of the reaction

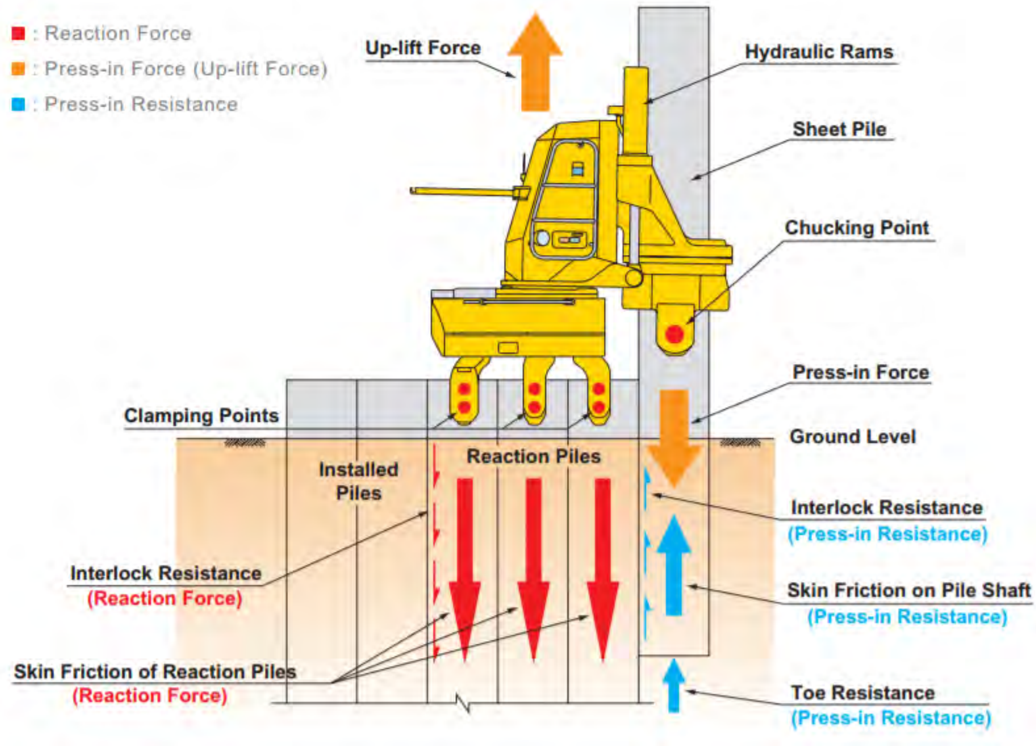

Figure 4: 'Press in' Method
(Giken Construction Revolution Guide Vol.1, 2001)

forces and allows a self-moving installation procedure to finish construction of a sheet pile pit in one go. The self-moving process is shown in Fig 5. The hydraulic ram along with chuck is able to rotate, which also enable curve installation of sheet piles and the installation of piles at corner of a pit.

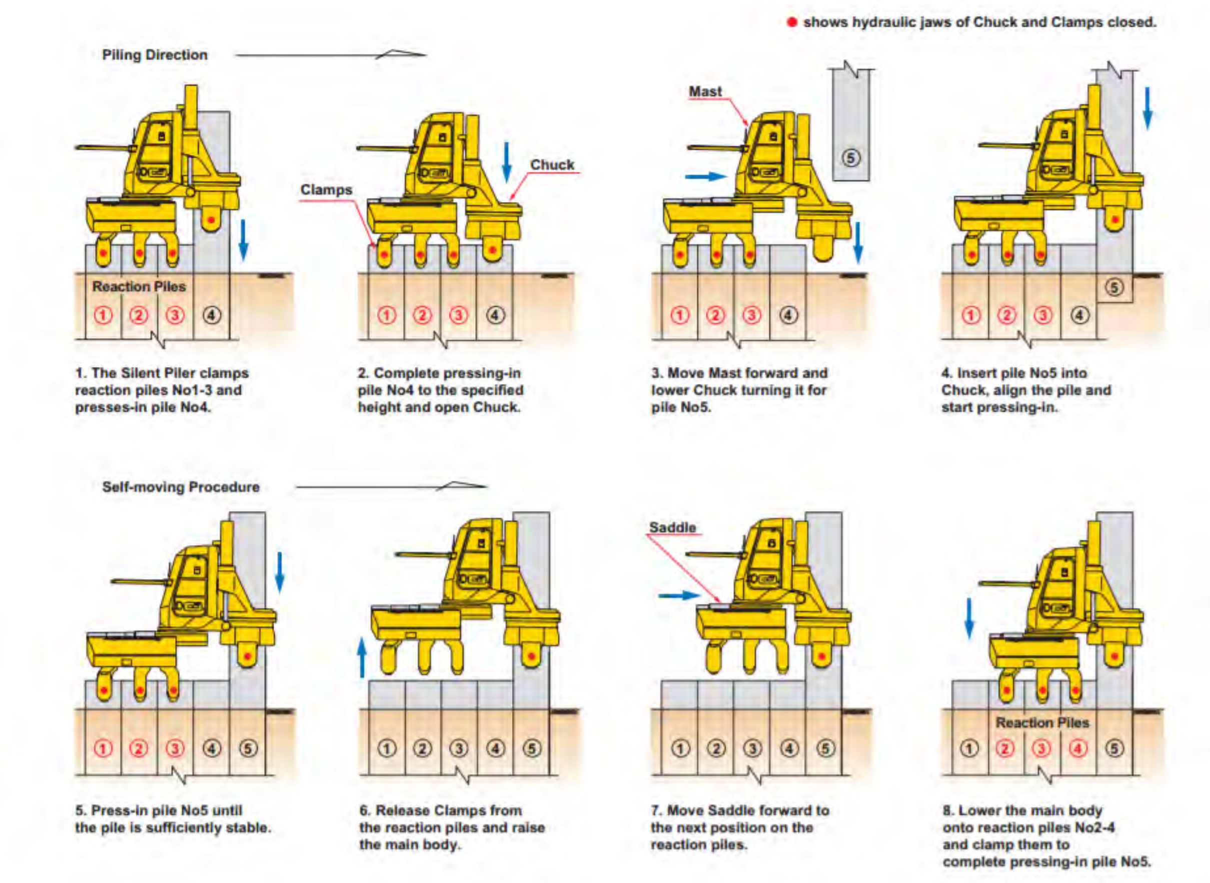

Figure 5: Self-moving mechanism
(Giken Construction Revolution Guide Vol.1, 2001)

2.2 Sheet pile properties

In order to construct a closed pit, series of sheet piles connected at interlocks at required. The type of sheet piles used in this project are shape NS-SP-IV with dimensions shown in Fig 6 (Nippon Steel & Sumitomo Metal, Sheet piles, 2012). Fig 7 shows that the interlock allows certain degree of rotation, which will decrease the bending stiffness of the sheet pile wall because the sheet piles can just move by rotating about the interlock. This issue has to be taken into account during analysis of the deflection of the sheet pile wall.

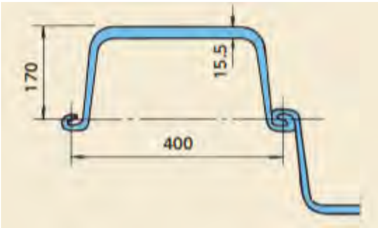

Figure 6: NS-SP-IV sheet pile dimension

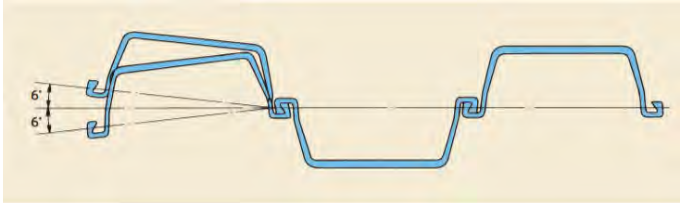

Figure 7: Sheet pile interlock rotation

2.3 Sheet pile structural analysis

Instrumented piles can be installed to give data about its structural behaviour, measurement of strain or inclination of the pile is possible. Because of the existence of interlocks between adjacent piles, the structural analysis is not straight forward. The interaction between piles, soil and interlocks have to be taken into account. (Kazusue Konoike, 1988) has suggested a way to calculate the bending moment of sheet pile wall based on strain gauge data.

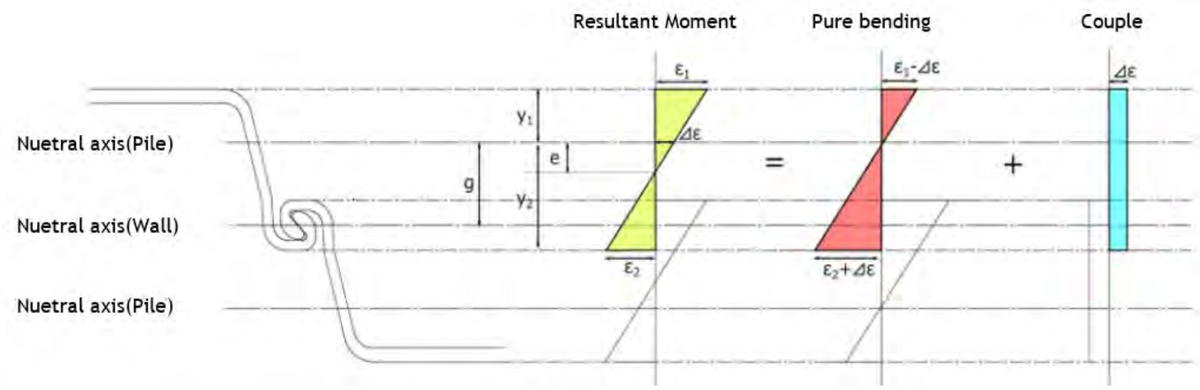

Figure 8: Bending moment calculation using strain value (Kazusue Konoike, 1988)

As illustrated in Fig 8, in order to calculate the bending moment of the sheet pile wall, an adjacent pair of piles should be considered. the resultant bending moment equals a pure bending about the neutral axis of each pile and a couple caused by the interaction between pile surface friction and the interlock. At least two strain gauges on each pile are required to work out the resultant neutral axis, so that components of resultant bending moment can be calculated. For the strain distribution we have:

$$\frac{y_1 + e}{\varepsilon_1} = \frac{y_2 - 3}{\varepsilon_2} \tag{1}$$

Rearrange we have:

$$e = \frac{y_2\varepsilon_1 - y_1\varepsilon_2}{\varepsilon_1 + \varepsilon_2} \tag{2}$$

Similarly we can deduce:

$$\Delta\varepsilon = \frac{e}{e + y_1}\varepsilon_1 \tag{3}$$

The magnitude of the couple will be:

$$Couple = gEA\Delta\varepsilon \tag{4}$$

Bending moment generated due to pure bending on each pile can be calculated using simple beam theory:

$$M = \frac{\sigma I}{y} = \frac{EI}{y_1}(\varepsilon_1 - \Delta\varepsilon) \tag{5}$$

By combining Equation 4 & 5, the total bending moment is:

$$M = \frac{\sigma I}{y} = \frac{EI}{y_1}(\varepsilon_1 - \Delta\varepsilon) + gEA\Delta\varepsilon = \frac{E(I + egA)}{e + y_1}\varepsilon_1 \tag{6}$$

Apart from obtain bending moment from strain gauges, inclination measurement will also allow bending moment calculation. By using two methods together, more reliable results can be achieved.

2.4 Soil pressure distribution

Rankine Theory and Mohr Coulomb Theory are the two most used theories to calculate the soil pressure acting on a retaining structure. Rankine's Theory assumes the wall is frictionless and the soil is homogeneous, isotropic and has internal friction. The pressure exerted by the soil on the wall is referred as active pressure and the resistance pressure offered by the soil is referred as passive pressure. The failure envelope for passive and active soil are shown in Fig 9 & Fig 10.

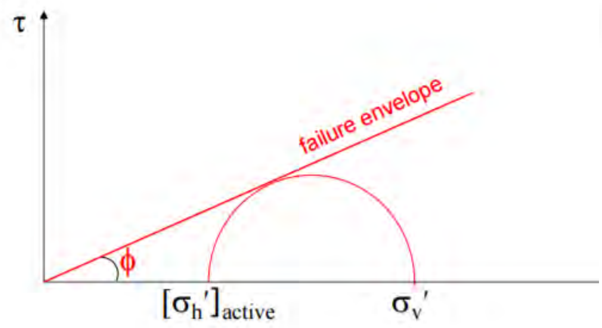

Figure 9: Active failure envelope

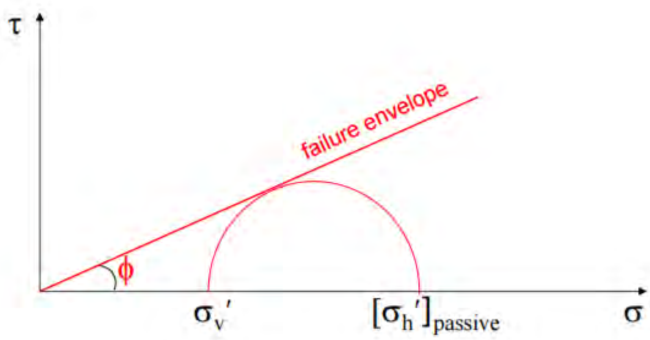

Figure 10: Passive failure envelope

ϕ is the soil friction angle, which can be obtained from direct shear test. K_a and K_p are coefficient for active and passive soil pressure can be defined based on the failure envelope.

$$K_p = \frac{1 + sin\phi}{1 - sin\phi} = tan^2(45 + \phi/2) \tag{7}$$

$$K_p = \frac{1 - sin\phi}{1 + sin\phi} = tan^2(45 - \phi/2) \tag{8}$$

The lateral soil pressure can then be calculated using these factors, and triangular distribution of soil pressure is assumed.

$$[\sigma'_h]_{passive} = K_p\sigma'_h + 2c\sqrt{K_p} \tag{9}$$

$$[\sigma'_h]_{active} = K_a\sigma'_h - 2c\sqrt{K_a} \tag{10}$$

Where c is the cohesion of the soil, and c = 0 in granular soil. If the cohesion is too big, the soil will stand on its own, there will be hardly and active pressure applied onto the wall. Rankine's Thoery is only valid on vertical walls.

Mohr Coulomb Theory was established on the basis of the equilibrium of forces on the whole sliding wedge of soil and gave the resultant earth pressure (Limit equilibrium theroy). The limiting horizontal pressure at failure in extension or compression are used to determine K_a and K_p respectively. A linear distribution of soil pressure is also assumed during practical application of Mohr Coulomb's Theory. However various studies indicated that the distribution of pressure will depend on the mode of movement of the wall. (Wang, et al. 2004) suggested that in sliding stability analysis, Mohr Coulomb Theory can be used to calculated the resultant soil pressure, while in overturning stability analysis the effect of failure mode has to be taken into account.

2.5 Laboratory determination of soil properties

Soil properties such as friction angle ϕ and cohesion c can be drived through laboratory sample testing. Direct shear test is the most common one. Shear box tests on a soil sample under at least three different normal stress are required. The results are plotted on a graph of shear stress against normal stress, and a best-fit line is drawn through the peaks, which is known as Mohr-Coulomb strength envelop and it is defined by Equation

$$S = Ntan(\phi) + c \tag{11}$$

Where S is the shear stress, N is the normal stress. Based on this best-fit line, soil friction anlge and cohesion can be found. However, according to the arguement in (Richard Thiel, 2009), the best-fit line should not be extrapolate beyond the limit of normal stress that the direct shear test is conducted, because the real envelope should be curved. As shown in Fig 11, the actual envelop may have a smaller intersection with vertical axis. It means the actual cohesion of soil may be much smaller than that obtained from the best-fit line.

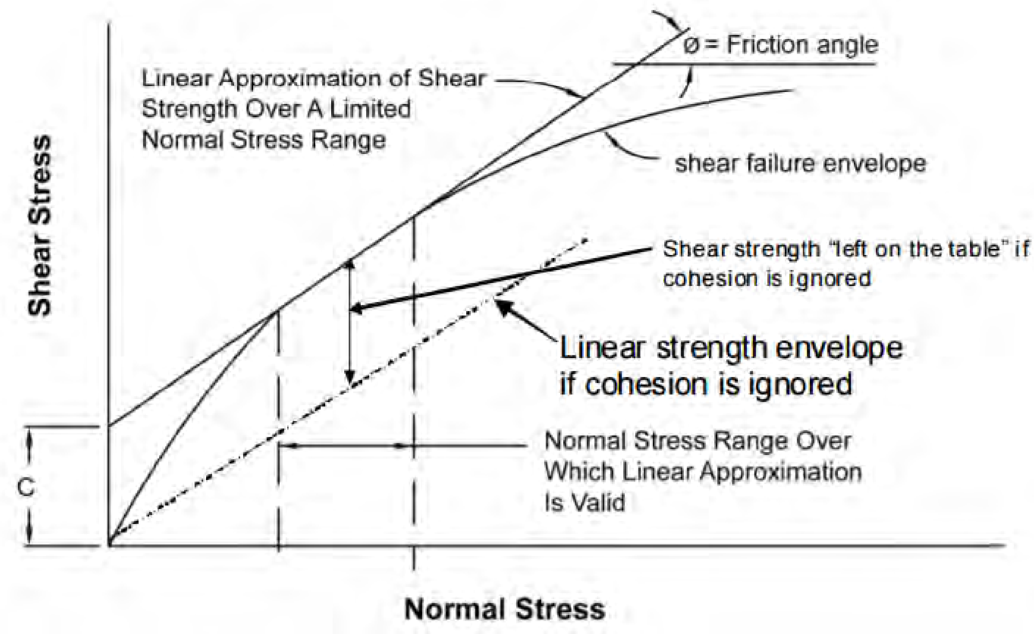

Figure 11: Exaggerated Schematic of True Curvilinear Shear Strength Envelope, Linear Interpretation over a Selected Normal Stress Range, and the Penalty for Ignoring Cohesion
(Richard Thiel, 2009)

2.6 Friction fatigue on jacked pile

D. J. White & M.D. Bolton (2002) did calibration chamber testing combined with displacement measurement with image analysis to analyse the mechanism of a jacked pile. It is observed that the soil adjacent to an advancing pile revealed the movement towards the shaft and this movement is linked to the decrease in horizontal stress acting on the pile, which is known as 'friction fatigue'. D. J. White & M.D. Bolton (2002) suggested the continuous shearing at the soil-pile interface will cause reduction in volume in the zone of soil close to the pile, this reduction permits soil further from the shaft to relax and cause decrease in horizontal stress and hence shaft resistance of the pile. Fig 12 illustrates the mechanism.

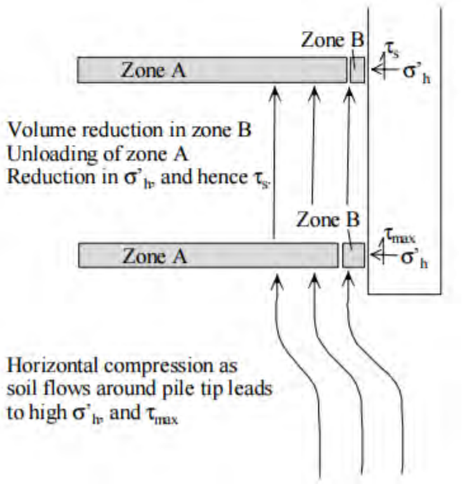

Figure 12: Friction fatigue mechanism
(D. J. White & M.D. Bolton, 2009)

2.7 Retaining wall

2.8 Finite element analysis on retaining wall

2.9 Ground inprovement

3 Field testing

3.1 Goals

Field tests on two sheet pile pits with different dimensions were designed to analyse the structural behaviour of sheet pile walls during different construction stages, including bottom stabilisation and excavation. The structural behaviours to be investigated include:

1. Deflection of sheet pile wall during stabilisation and excavation processes.
2. Bending moment change in sheet pile wall during stabilisation and excavation processes.
3. The prop load variation during excavation.

The goal of these field tests is to preliminarily understand the effect of bottom stabilisation and structural behaviour of the pit during excavation. The structural behaviour results will be compared with finite element modelling which will be carried out later.

3.2 Sheet pile wall installation

The sheet piles are installed using the GRBS method mentioned in Section 1.1. GRBS method is also known as 'Press-in' method and a pictures illustrates the installation method is shown in Fig 4 and Fig 5 in Section 2.1. The silent piler model ECO-1OO was used to construct the sheet pile pits used in these field tests. As discussed in Section 2.1 the self-moving mechanism and the curve installation technology allow construction of a pit in one go.

Figure 13: Sheet pile pit on site

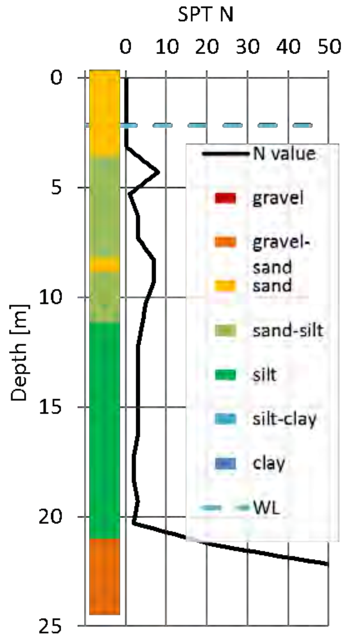

Figure 14: SPT result of test site

Two pits with dimensions shown in the Table 1. were built and the plan views are shown in Fig 15. The No.1 pit finished construction on 10^{th} of July 2016 and No.2 pit finished construction on 24^{th} November 2016 on Giken Kochi Headquarters Test Field in Kochi Japan. Fig 13 shows the finished construction of pit 1. The SPT results of the test site is shown in Fig 14, the soil is mainly silt. Piles at several locations are instrumented, which allow continuous collection of data during different construction stages. More information of the sensors used to collect data will be discussed in Section 3.4. The structural behaviour of these two pits will be analysed and compared.

3.3 Bottom stabilisation and excavation

The bottom stabilisation process is carried out on pit 1 directly after the construction while pit 2 will not be stabilised. The process is done by Giken 'press-in' machine model SCU-ECO400S. The machine shown in Fig 16 equipped with an auger is able to remove soil and pour concrete grout into desired depth. The stabilisation aims to improve the soil between a depth of 9.5 m to a depth of 12.5 m by pouring concrete to form columns with diameters about 500 mm. The layout of the columns is shown in Fig 17. The whole stabilisation process takes about 20 days from 23_{th} July to 12_{th} August. Because it is

	Pit No.1	Pit No.2
Dimension	8.4×6m	8.4×8.4m
Depth	16.5 m	10 m
Pile type	SP-IV	SP-IV

Table 1: Dimension of two pits

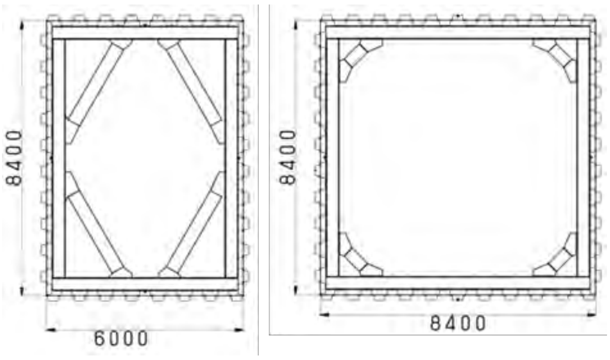

Figure 15: Pit 1 (Left),pit 2 (Right) (in mm)

a new construction method and is just developed, various issues delays the construction process. If the stabilisation is proved to be effective, the construction method may be improved and the time taken to finish the stabilisation can be much shorter in the future.

Figure 16: Model SCU-ECO400S

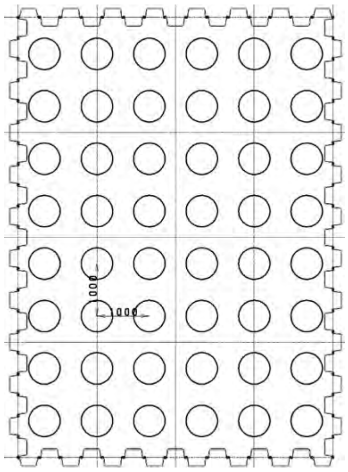

Figure 17: Stabilisation layout

The stabilisation process involves three steps and are summarised in Fig 18. The auger is first been driven into aimed depth by the 'Silent Piler' and concrete is pumped in to the auger by concrete pump. The valve at the bottom of the auger can be controlled remotely. Concrete is poured by opening the valve and meanwhile the auger is lifted up by the 'Silent Piler' to allow formation of the concrete columns. The hole above the column is filled by soil and the next column is then going to be constructed. Such operations are repeated to finish the stabilisation layout of pit 1 illustrated in Fig 17 after which the excavation process will start.

Excavation of pit 1 started on 8^{th} September and finished on 27^{th} September 2016 and the excavation of pit 2 started on 2^{nd} December and finished on 10^{th} December 2016. Props are installed to support the sheet piles in order to prevent large deflection. The excavation procedure for pit 1 & 2 including prop installations can be summarised below. For pit 1

1. 1.5 m excavation

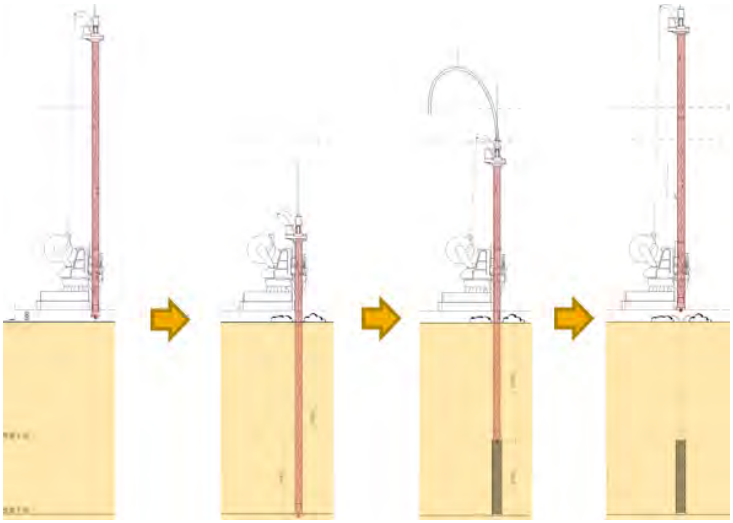

Figure 18: Stabilisation process

2. Install first prop at ground level
3. Excavate to 4 m
4. Install second prop at 3 m below ground level
5. Excavate to 7.5 m depth
6. Install third support at m below ground level
7. Finish excavation up to 9.5 m

For pit 2

1. 1.5 m excavation
2. Install first prop at ground level
3. Excavate to 4 m
4. Install second prop at 3 m below ground level
5. Finish excavation up to 5 m

Fig 19 shows the photo of stabilisation columns after the excavation of 9.5 m.

3.4 Sensors and data collections

In order to measure the deflection of the sheet pile, inclinometer is used to measure the inclination of the sheet pile wall at different depth. Four square hollow section tubes are attached onto the middle sheet pile on each side for both pits, total station lens are also

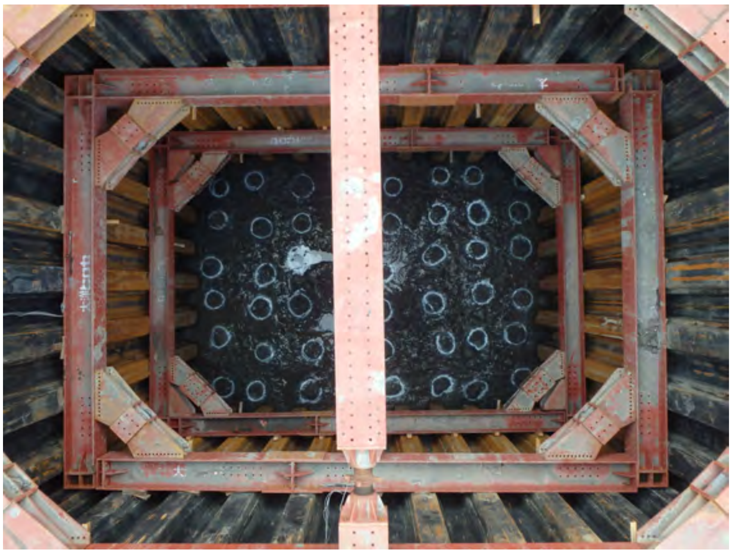

Figure 19: Finished stabilisation

attached at the same positions to track the pile head displacement continuously. Total station will measure the movement of the pile head every 15 minutes and the results are logged automatically. The plan view of the field test site are shown in Fig 20. The position of the total station will be checked manually every morning against another reference point far away.

When measuring the inclination of the pile, the inclinometer in Fig 22. was first inserted into the square hollow section tube and lowered to the bottom. The inclinometer is then pulled up 20 cm each time, a digital reader will record the reading at these positions. The inclination will be measured with positive and negative orientation of the inclinometer, the difference of the two readings multiplied by the calibration factor will be the inclination of the pile, by doing this the error of inclinometer can be cancelled, and a more accurate result can be obtained. The measurement will be carried after the stabilisation or excavation work everyday at about 6 pm and usually 15 minutes will be used to measure the inclination of a single pile.

Figure 21: Hollow section tube

Figure 22: Inclinometer

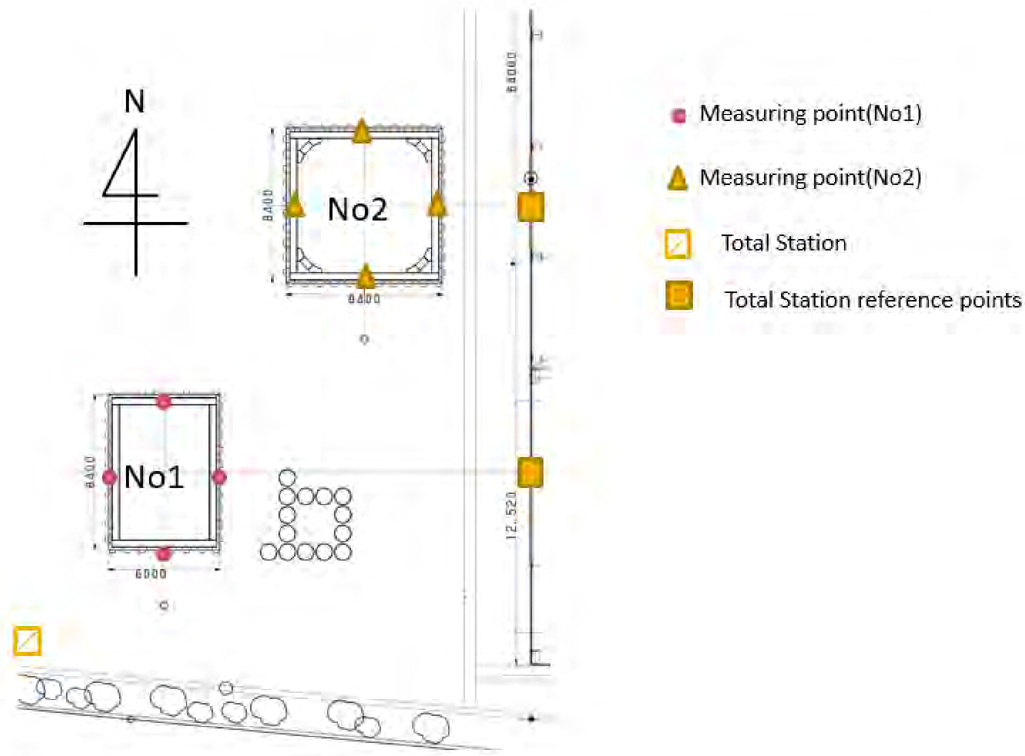

Figure 20: Inclination measurement and total station postion

Apart from measurement of inclination, strain gauges are also embedded on piles adjacent to the hollow section tube at different depth on north side wall for pit 1 and west side wall on pit 2 (North is defined in Fig 20), which can also be used to deduce the bending moment as well as deflection of the pile. The results will be compared with inclination measurement in later sections. Water and earth pressure sensors are also embedded on the piles on north side wall for pit 1 and west side wall on pit 2. However, water pressure sensors near bottom of the pile are found to be broken during the stabilisation process. The positions of these sensors are summarised in Fig 23.

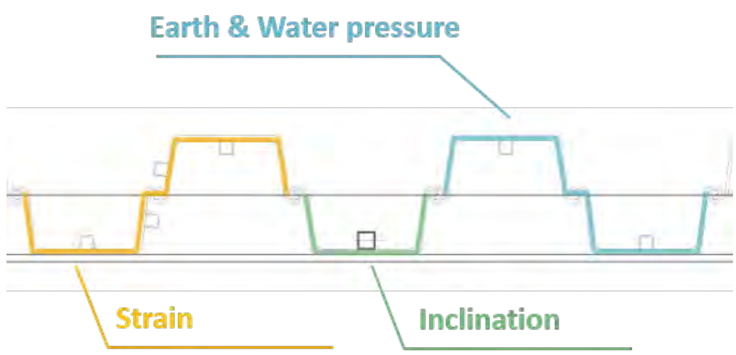

Figure 23: Sensor postitions

The depth of all the sensors are shown in Fig ??, which is a cross section of these two pits after excavation, the positions of props and stabilisation zone are also shown in the figure. Except inclination measurement, all the other sensors will collect data automatically and they are logged continuously by the on-site computer.

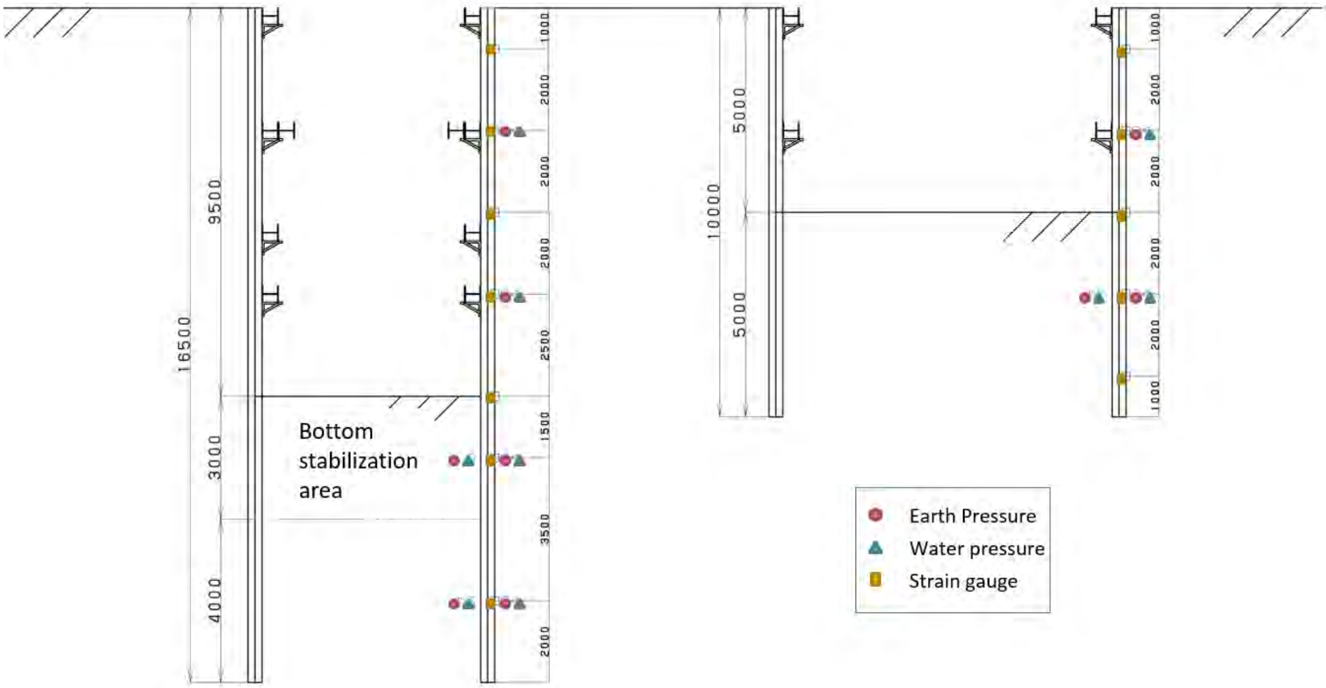

Figure 24: Sensor postitions

Strain gauges are also installed on all the structural components of the props, the layout of the sensor positions are shown in Fig ?? & Fig 26. Each dot represents a pair of strain gauges allow measurement of strain due to axial force and bending moment. The beam members used in the props have a section of Japan Steel 400×400×21×13 mm.

3.5 Field test results and discussions

3.5.1 Deflection shape

Based on beam theory, the deflection of the piles can be obtained by numerical integration of the inclination data, which is measured at 20 cm interval along the pile. The total station measurement will be used as a boundary condition to make sure the pile head displacement is the same as the total station measurement.

$$\Delta = \int \Theta dz \tag{12}$$

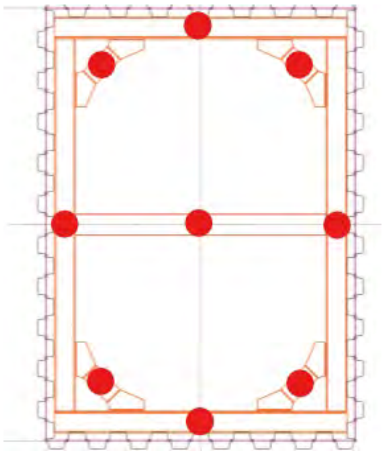

Figure 25: Pit 1 prop strain gauge positions

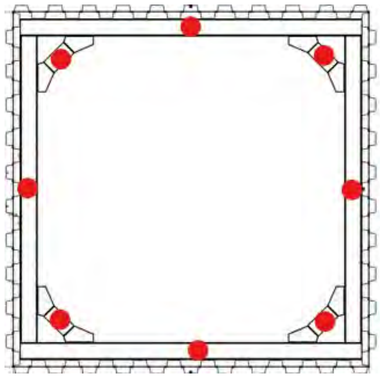

Figure 26: Pit 2 prop strain gauge positions

The change in deflection of the piles on North side of pit 1 and West side of pit 2 after the construction of the pits are shown in Fig 27 & Fig 28. The blue lines are the positions of the props and red lines are the positions of excavation level.

Comparing to pit 2 deflection shape, the pit 1 deflection shape shows clearly that the pile near stabilisation zone which is 9.5 m below ground level is significantly pushed outwards the pit. As discussed previously, since extra materials are added into the stabilisation zone and extra horizontal stress is also applied during this process. Pit 1 shows a larger deflection during excavation process, because the excavation depth is larger than pit 2. Referring to the excavation process stated in Section 3.3, the time of prop installation is known, however, according to the deflection plot piles still allowed to move even after the installation of props. Giken, the company in charge of the construction process of the whole test admitted that there are gaps left between the props and the pile wall and it is the main reason cause this problem. From the deflection during excavation process, gaps about 1 to 2 cm may exist in pit 1, the size of the gap may make the props useless. Detailed analysis on prop load will be discussed in later sections.

3.5.2 Pit 1 Bending moment

Bending moment distributions in the piles are obtained from inclination measurement by differentiating the inclination data. Based again on beam theory:

$$M = \frac{1}{EI_{permeter}} \frac{d\Theta}{dz} \tag{13}$$

The second moment of area of the pile wall used is based on the data given by the manufacturer these information is summarised in Table 2.

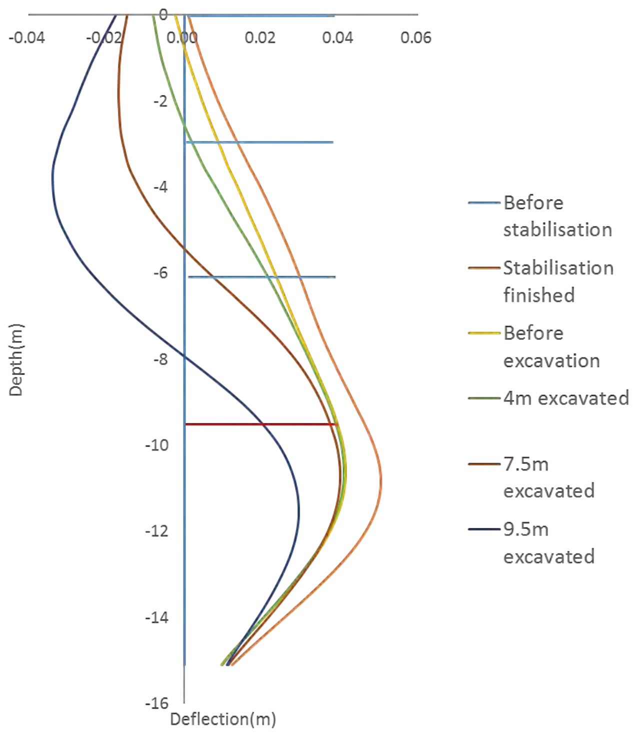

Figure 27: Pit 1 deflection (positive is outwards the pit)

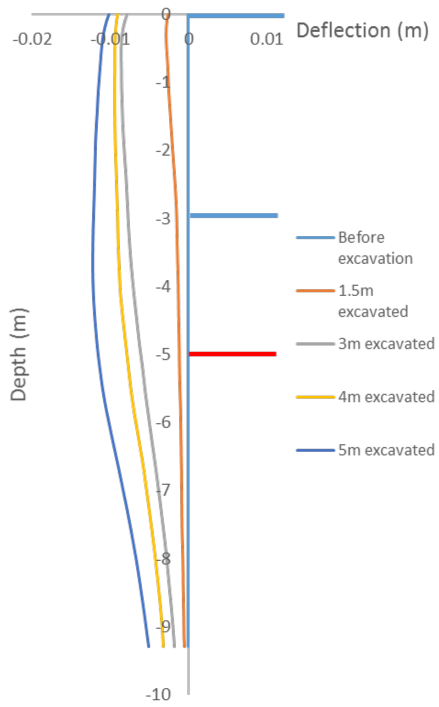

Figure 28: Pit 2 deflection (positive is outwards the pit)

Table 2: Dimension of two pits

	Weight (kg)	Cross section area (m^2)	Second moment of area (m^4)
Per pile	76.1	9699×10^{-6}	467×10^{-7}
Per meter	190	2425×10^{-5}	386×10^{-6}

The bending moment distribution of pit 1 calculated using inclination data are shown in Fig 29 & Fig 30. Fig 29 shows the bending moment change since stabilisation and Fig 20 shows the bending moment change during excavation process. The highest bending moment above the excavation level is about 125 kNm/m, which corresponding to a stress of only about 55 MPa at extreme fibre. It is much lower than the yield point of 295 MPa, so bending moment won't govern the design of such pit and deflection may be the governing factor. The top three blue lines in these Figures represent the props. The second support which is 3 m below the ground surface is installed after 4 m excavation, if the prop works properly, the bending moment will tend to change sign at the position of the prop, however the measured value tells a different story. These props didn't work as expected, as discussed in the previous section this may be caused by the existence of gaps between wall and props.

Bending moment value in these field tests can also be calculated using the strain gauge

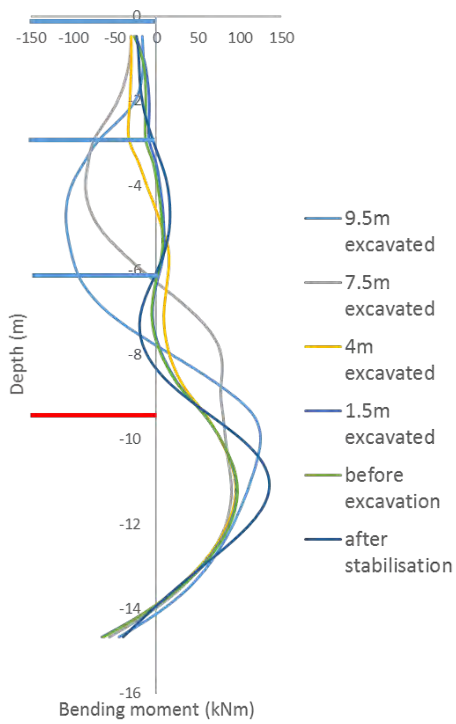

Figure 29: Pit 1 bending moment change after installation

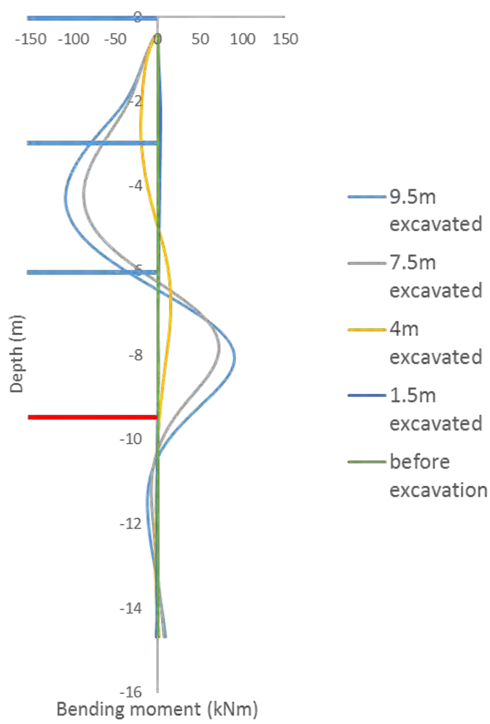

Figure 30: Pit 1 bending moment change since excavation

data. However, the calculation is not straightforward because of the existence of the pile interlocks. As discussed in Section 2.3. The resultant bending moment consists of two parts, the first part is the pure bending of the pile and the second part is a couple generated by the force at the interlock and the soil friction, which can be seen in Fig 8 in Section 2.3. Because of the existence of the couple, the real neutral axis of bending

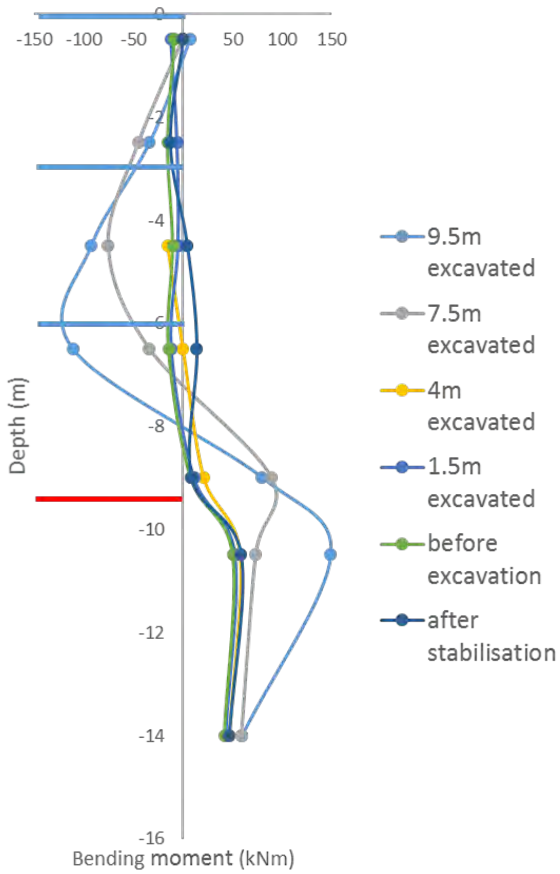

Figure 31: Pit 1 bending moment change after installation

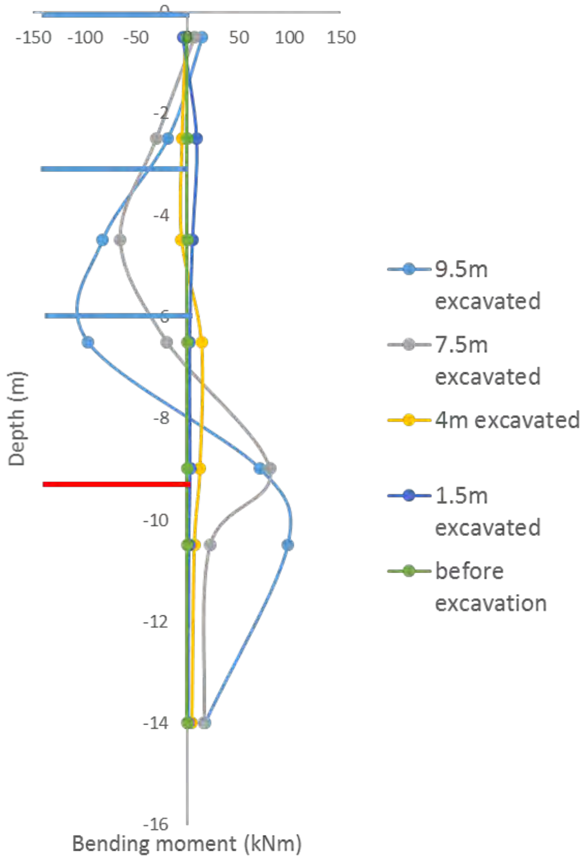

Figure 32: Pit 1 bending moment change since excavation

for each single pile has to be found using the strain gauge measurement. The two strain gauges on each pile shown in Fig 23 will be used to find out the neutral axis of bending on the adjacent piles. The bending moment one each pile can then be calculated using Equation 6 derived in Section 2.3. The second moment of area should use the value for each pile rather than the per meter value. The bending moment of two adjacent piles will then be added together under prescribed sign convention and the real bending moment per unit length will be the sum divided by the width of two piles, which is 0.8 m. The plot of bending moment calculated by this method is in Fig 31 and Fig 32.

Again Fig 31 shows the bending moment change since stabilisation and Fig 32 shows the bending moment change since excavation. Both diagrams show a higher bending moment value at near the bottom of the pile after 9.5 m excavation comparing to the bending moment at that position before. The big change in bending moment at that position shown in the graphs may caused by the data fitting, because there is no strain gauge between 9 m and 10.5 m, other peak bending moment may occur in between this range in earlier excavation process, but not captured by the strain gauges. Generally the strain gauge values also gives similar bending moment values. Comparing Fig 30 andFig

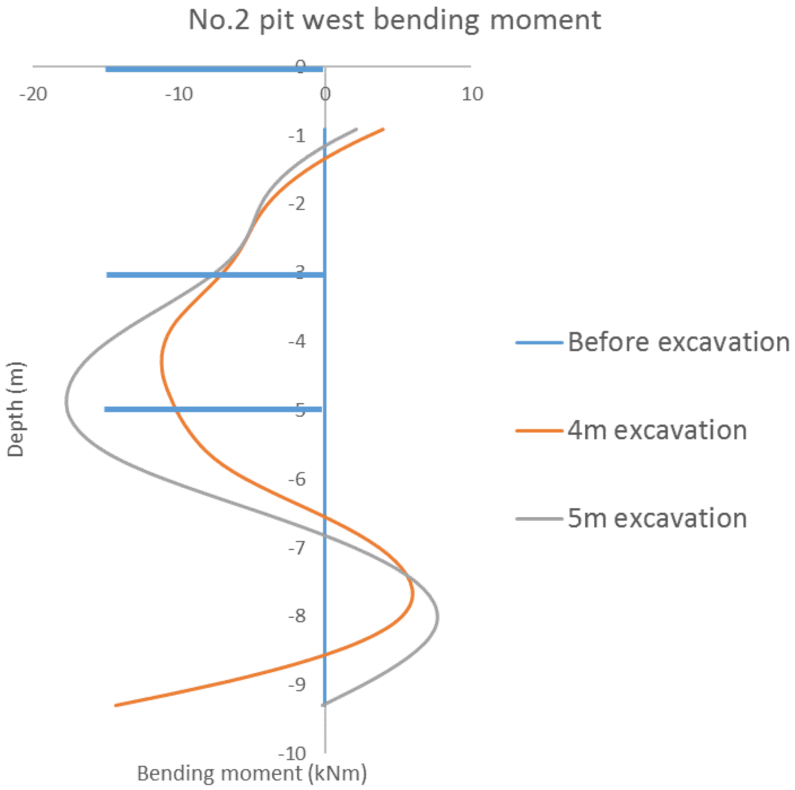

Figure 33: Pit 2 bending moment distribution

32 will gives an assessment on how these two method match with each other. The bending moment calculated by both methods all lies between the range from -120 to +100 kNm/m and the shape are almost the same, so the results obtained by both methods can be treated as consistent. One point needs to be mentioned is that for the '9.5 m excavation' curve, the position of the peak bending moment calculated by strain gauge method is deeper than that calculated by inclination method. If the change in bending moment since stabilisation is compared (i.e. compare between Fig 29 and Fig 31) the '9.5 m excavation' curves are found to be more similar. The reason of this observation also may be caused by data fitting on strain gauge method below 11 m. Otherwise these two methods gives reliable results on bending moment distribution and both show that the bending moment in the pile is much lower than yield point.

3.5.3 Pit 2 bending moment

The bending moment distribution of pit 2 is calculated using the same method as pit 1. However the strain gauges on excavation side at depth of -1, -3 and -5 m are broken due to unknown reasons, bending moment distribution cannot be calculated based on strain gauge data for pit 2. The bending moment distribution based on inclination measurement is shown in Fig 33.

The bending moment shape is similar to pit 1 while the magnitude is much smaller, which is expected, because the excavation depth is much lower. A bulge in bending moment near the second prop can be observed, which shows a more tight connect between props and wall is achieved during the construction of pit 2.

3.6 Prop loads and thermal effect

As mentioned in section 3.5.2, gaps may exist between props and sheet pile wall. In order to prove this, a simplified retaining wall calculation has been done to work out the loads in first prop (Top prop in pit 1 shown in Fig 24). The following assumptions have been made:

1. Based on previous bending moment diagram the point of zero bending moment is 10.5 m below the ground surface.
2. Soil unit weight is taken to be 18 kN/m^3.
3. Assume drained behaviour.
4. Water table is at ground surface.
5. Assume friction angle of soil equals 30°

The diagram in Fig 34 & Fig 35 shows the simplified analysis.

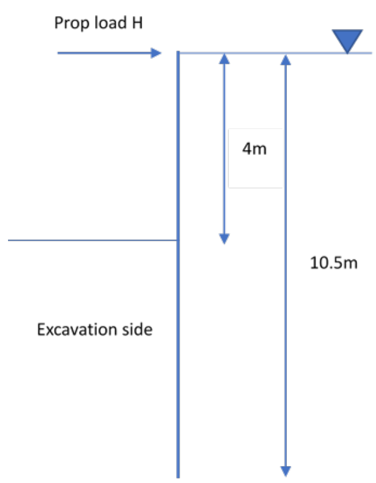

Figure 34: Pit 1 retaining wall

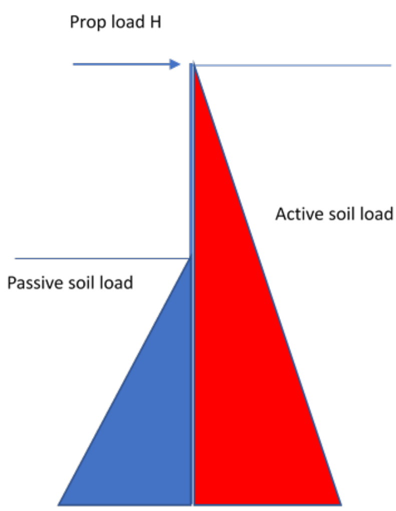

Figure 35: Pit 1 retaining wall loads

By considering horizontal equilibrium and moment equilibrium about the point of fixity the prop load H is 29 kN/m. The distributive load are applied on the prop circumferentially in a SAP2000 model and the resultant deflection shape and bending moment distributions are shown in Fig 36 & Fig 37. The bending moment at mid span on short and long side of the prop are 110 and 41 kNm respectively, these values are compared with the value calculated based on the strain gauge embedded onto the prop beams. The data at 23:00 on 15/09/2016 after the 4 m excavation is chosen to compare, because the zero reading of these strain gauges are set at night when the temperature is low. The measured value is much smaller with 4.2 kNm on short side and 12.4 kNm on long side. The simplified calculation is much bigger than the measured value. The estimation of soil weight and friction angles may be inaccurate, however the difference won't be that big. The existence of gaps can be proved.

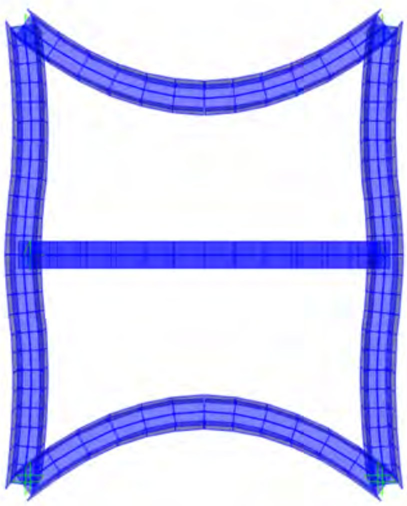

Figure 36: Prop deformed shape

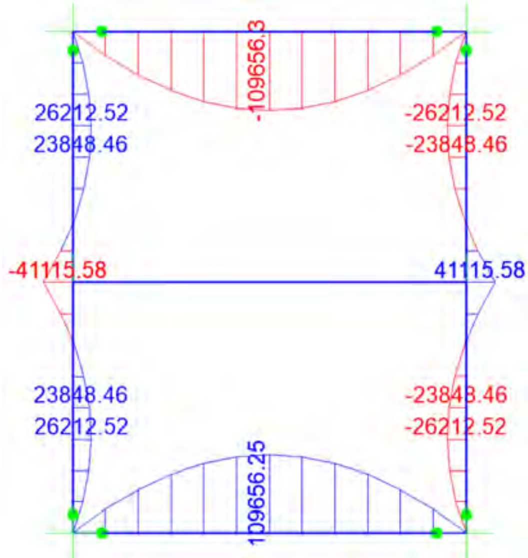

Figure 37: Prop bending moment (in Nm)

The variation in axial load of the middle beam (middle beam in Fig 36) with the excavation process is plotted. A huge daily variation in axial load can be observed. The field test took place in mid summer in Japan, the daily variation in temperature can exceed 10 °C. Because it is proved that gaps exist in between piles and props, the prop may free to expand, which means the load during day time in the prop may not be real load caused by the excavation process. If we focus on the axial load at mid night we can see a trend that the axial load of the beam is becoming more negative (more compressive) with the excavation process, which is as expected. Fig 38 shows that the daily variation in temperature may make the prop drive the pile wall back and forth if the prop is fully constrained by the wall.

The thermal effect on props is significant. Because no extra strain gauges are installed to calibrate the thermal expansion, it is difficult to calculate the actual reaction provided by the props. Further studies in thermal effect on props may be interesting, because if no gaps are left between piles and props, the strain in props caused by daily variation in temperature may apply load on the pile and hence move the pile back and forth. The load may not be big, but if accurate analysis on structural behaviour of pile is required, this effect can not be ignored.

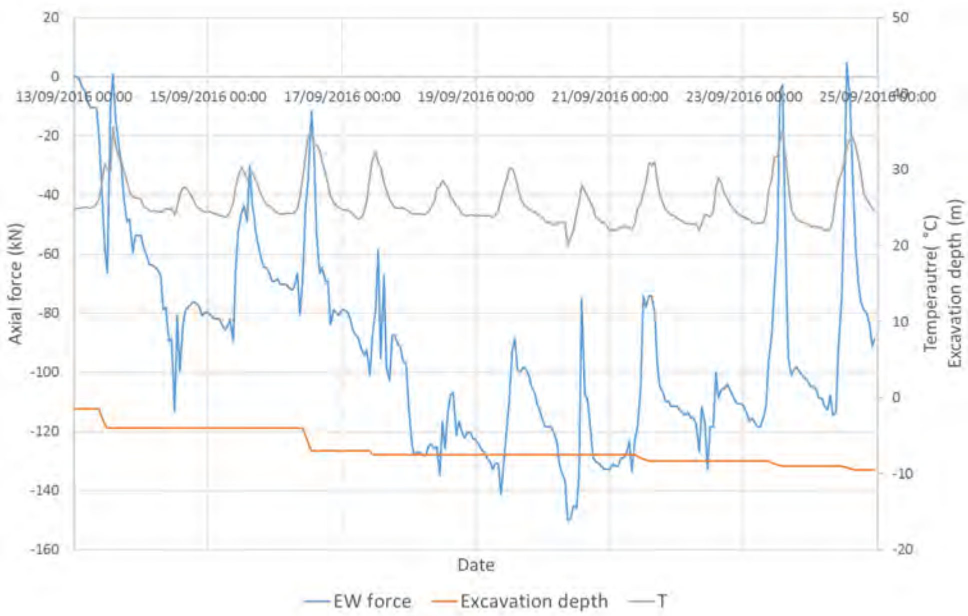

Figure 38: Prop middle beam axial load variation

3.7 Achievements and Difficulties

Good field test data have been obtained and analysis on the structural behaviours have been done. The deflection and bending moment distribution of the pits are as expected. As mentioned in Section 1.2, the field test results show that the stabilisation process deflects the wall and applies extra bending moment in the piles. The main purpose of the project is to assess the effect of ground improvement on the stability of the pit, however, because the dimensions of pit 1 and 2 are different, a direct comparison between these 2 pits cannot be done only based on the field test results. Apart from this, the gaps existing between props and wall makes the effect of props more difficult to analyse, the props cannot be treated as rigid supports not be ignored. Further numerical modelling analysis should be done to analyse the behaviour of the whole pit. Comparisons between field test results and FE modelling results will be conducted, and the effect of bottom stabilisation will be analysed by comparing the behaviour of the models with and without bottom stabilisation.

4 Finite Element Modelling

4.1 Goals

Because different dimensions of two pits in field tests, direct comparison between behaviour of pits with or without bottom stabilisation cannot be done. Apart from this, the 3D effect of the pit cannot be analysed based only on the field test data, because sensors only tell the behaviour of a single pile. Finite Element Modelling is introduced to solve these problems, because FEM has the following advantages:

1. Allow 3D analysis.
2. Allow change in material properties and dimensions easily, so that different analysis can be done to address design suggestions.

The goals of FE modelling are:

1. Analyse 3D behaviour of the pit.
2. Comparing structural behaviour of models of pits with and without bottom stabilisation.
3. Change material properties and analyse the difference in behaviour
4. Come up with design suggestions.

ABAQUS CAE is used for the Finite Element Analysis.

4.2 2D retaining wall modelling

It is difficult to build the model of whole pit in the first trial, so a single side of the pit is modelled first. The north side of the pit 1 is chosen, because it is where most of the sensors are located and the structural behaviour of the mid pile on this side was discussed in Section 3.5.2. The whole wall is modelled as a isotropic steel shell with thickness of 6 cm, width of 6 m and 16.5 m deep. Full excavation of 9.5 m is assumed, which means the soil pressure is applied on active side of the wall between 0 to 16.5 m and on passive side between 9.5 m to 16.5 m. As discussed in Section 2.4 linear variation in soil pressure is assumed, and K_a is assumed to be 0.4 and K_p is assumed to be 2.5. The soil on passive side may not be fully mobilised and the value of K_p may be too big, however, at this stage the trial is just made to assess the effectiveness of the modelling, so the definitions of the soil properties are not important. The two long sides of the wall is hinged to model the 3D effect of the pit, because as shown in Section 2.2 the interlocks between piles allow a rotation up to 6°. The model was run and the results of deflection and bending moment are presented in Fig 39 & Fig 40.

Because it is just a trial of the modelling, the magnitude of the deflection and bending moment are not important. The deflection shape shows the pile above the excavation depth bulged inwards, which is as expected. The embedded part of the pile is bulging outwards, which is caused by the higher magnitude of the soil pressure on the passive side and it is not correct, because horizontal equilibrium is not achieved in this case. In the 3D modelling of the whole pit, the soil pressure will be replaced with real soil part

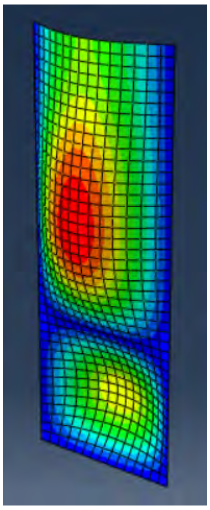

Figure 39: 2D modelling deflection shape

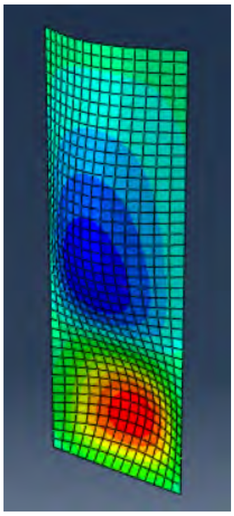

Figure 40: 2D modelling bending moment distribution

and such situation will not happen again. The bending moment distribution also shows similar behaviour as the bending moment diagrams in Section 3.5.2. These simple check make sure that the modelling of the pile should work and the 3D modelling of the whole pit can be started by replace the load applied by actual soil part.

4.3 Direct shear test on soil sample

Soil samples have been collected from Japan on the field test side. From the on-site CPT test result shown in Fig 14 the soil is classified as silt. The soil sample is obtained from soil from 9 m deep. Direct shear test on the sample was carried at CUED to find out the cohesion and friction angle. The method was described in Section 2.5. Three tests were carried with applied vertical stress equals to 100, 200 and 400 kPa respectively, consolidation was allowed before direct shear was taken place. The plot of shear stress against vertical stress of these three tests are shown in Fig 41.

The best fit line of the peak shear stress of these three tests are drawn. According to Equation 11 introduced in Section 2.5. The gradient of this best fit line will be the $tan\phi$ and the intersection with vertical axis is the cohesion c. The figure shows that the friction angle of this soil sample is about 22° and the cohesion is about 60 kPa. These values will be used as an initial soil property in FE modelling. However based on the discussion in Section 2.5, the real failure envelope is curved and the cohesion of soil may be much smaller, detailed discussion on choice of soil properties will be discussed later.

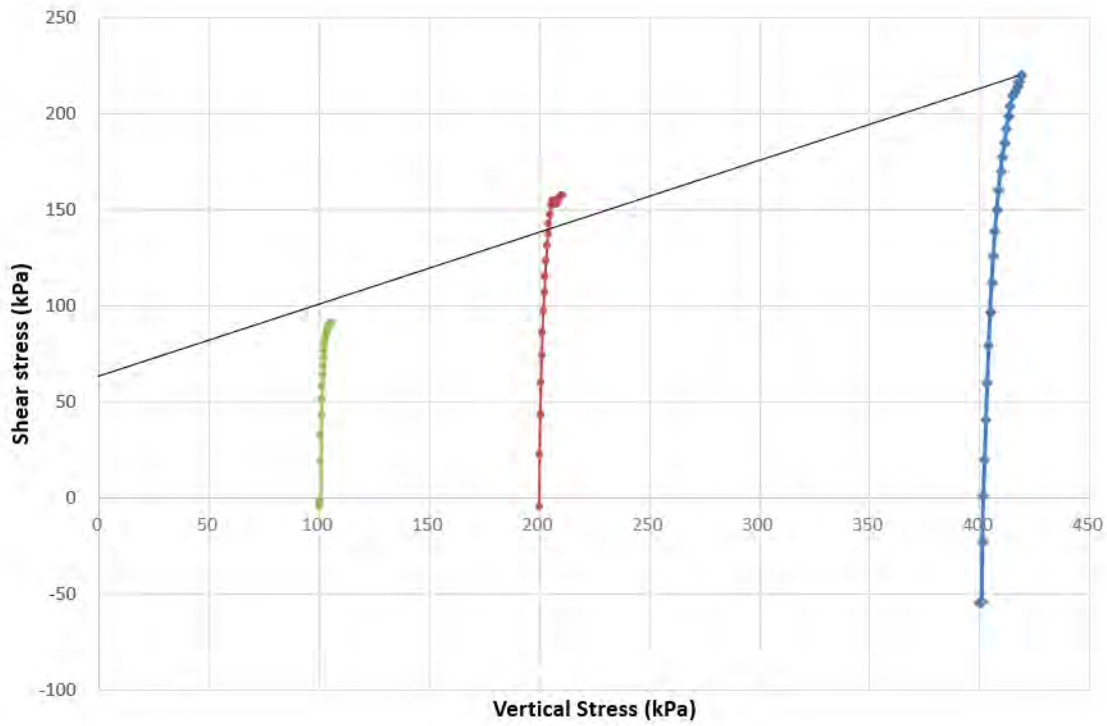

Figure 41: Direct shear test result

4.4 Pit 2 modelling

4.4.1 Initial model

FE modelling tells the true story only if sensible material properties are defined and correct boundary condition are set. Because the effect of bottom stabilisation is not known, it is impossible to model this effect in the model initially, however, the 3D model of pit 2 can be created first and the results will be compared with field test data in order to correct the material properties, because pit 2 is not stabilised. The sheet pile wall is again modelled as isotropic steel shell with thickness of 6 cm. The soil properties are summarised in Table 3.

Table 3: Soil properties

Friction angle	Unit weight	Cohesion	Voids ratio	Permeability
22°	20kN/m^3	60 kPa	0.7	0.0001 m^2

Props are not modelled in this case and 5 m excavation is done in one step and no props are modelled. The model consists of three parts: external soil, inner soil (excavated depth) and sheet pile wall. In order to simulate the excavation, initial pressure is applied on the inner side of the pile to simulate the state before excavation, the value of the pressure is chosen to ensure minimal initial deflection. This pressure is then removed in the next step to simulate the excavation of 5 meters. The outer soil part is modelled as a 20×20×20 m block with a central extrusion for piles and inner soil. The outer surface of the soil part is restrained to move. The size of the pit and inner soil level are all the same as field test.

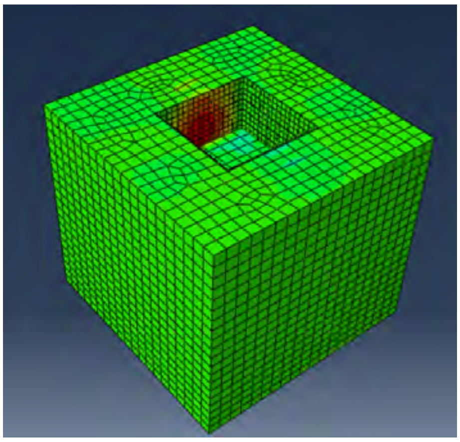

Figure 42: Pit 2 FE model

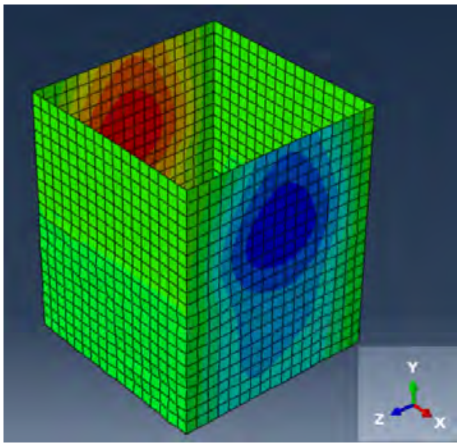

Figure 43: Pit 2 FE modelling deflection shape

Fig 42 shows the meshed model of pit 2 and the result of deflection of the sheet pile wall are shown in Fig 43. The deflection and bending moment results of this model are compared with field test results and shown in Fig 44 & Fig 45. The deflection shape of the model is very similar to the field test results, however the magnitude is only about half of the 5 m excavation field result. The bending moment predicted by the model is also smaller. Both results show that either the stiffness of the sheet pile wall is larger than the actual value or the cohesion is too big. As discussed in Section 2.2 the interlock between piles allow a rotation up to 6°, which will decrease the stiffness of sheet pile wall in bending about longitudinal axis significantly. The sheet pile property defined in this model is isotropic and the same stiffness is assumed for bending about both longitudinal and transverse directions. A new model should be created with reduced bending stiffness about longitudinal axis by defining the sheet pile wall as an anisotropic part. Additionally, the discussion in Section 2.5 also shows the actual cohesion may be much smaller than the value obtained from best fit line. Large cohesion values means the soil can stand on its own without applying much pressure onto the wall. Smaller cohesion values will be tried in order to get best fit with field test results.

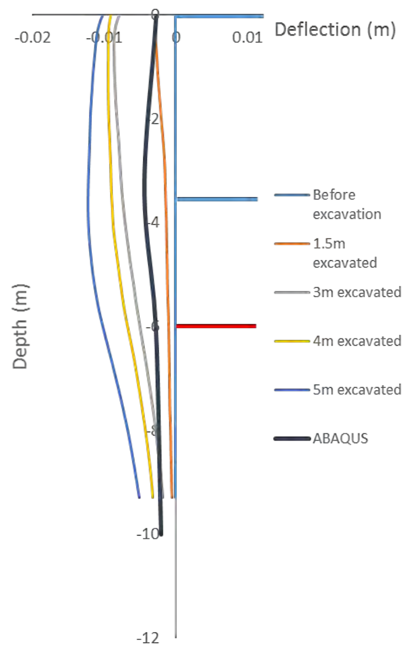

Figure 44: Deflection comparison

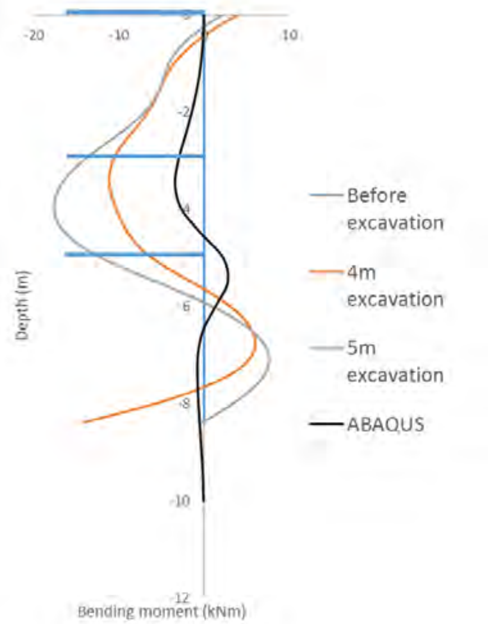

Figure 45: Bending moment comparison

4.4.2 Modified model

As discussed in the previous section, the material properties of the sheet pile wall part has to be modified. Additionally, the excavation process defined in Section 3.3 is going to be modelled including the effect props. Based on the discussion in Section 3.6, gaps existing between sheet pile wall and props are difficult to model because there is no information on how big the gaps are. In this finite element modelling the props will be modelled at rigid supports that stop further deflection of the wall at installed positions. In ABAQUS CAE, the props will just be modelled as boundary conditions that fix the position of the pile wall after the installation of the prop. Process of excavation is modelled by applying linear earth pressure distribution onto inner pile wall surface, which represents the reaction provided by the remaining inner soil. Different cohesion values have been tried to see the modelling results. If the 60 kPa value is used there will hardly be any deflection in the sheet pile wall and a much smaller value of 6 kPa is used in this model. The results of deflection is plotted in Fig 46 and is compared with the field test results shown in Fig 47.

The ABAQUS analysis results give a much smaller pile head deflection compared to the field test values. As discussed previously, the gaps between props and wall on site allow the pile wall to deflect after the installation of props, however, ABAQUS models these props by assuming they are rigid and won't allow any further deflection after installation. In Fig 46, it is clear that the pile head stops moving further after the installation of the

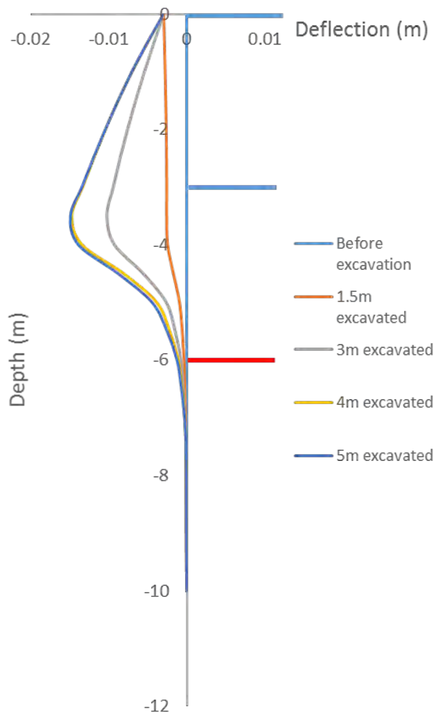

Figure 46: ABAQUS result

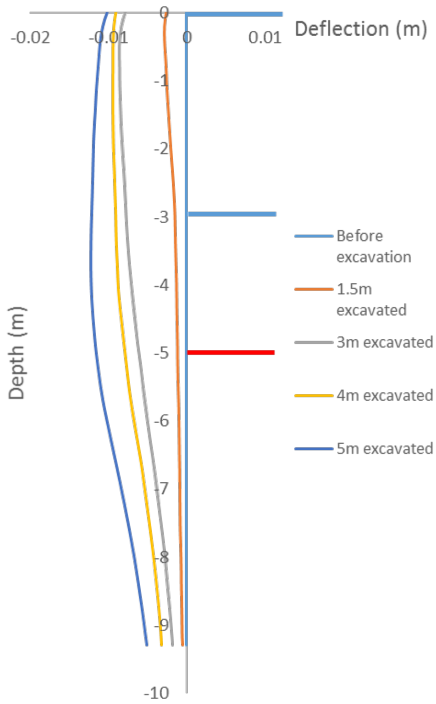

Figure 47: Pit2 field test deflection

first prop after 1.5 m excavation. The same applies to the second prop at -3 m depth. Another noticeable different is the deflection of the embedded part of the pile. The FE modelling shows there is hardly any deflection in the embedded part of the pile, while the field test result shows that at 5 m excavation the bottom of the pile moves 5 mm towards the excavation side. It may caused by the soil modelled is stiffer than that in reality. The real situation on site is really complicated, the installation of the pile involves surging, which moves the soil near the pile back and forth. Based on theory discussed in Section 2.6, the installation process may cause friction fatigue of the soil around the pile and decrease the lateral capacity, which may be the reason results in a noticeable deflection at the bottom of the pile. The ABAQUS results give a good estimation on the highest value of the deflection. The bending moment distribution is also compared with the field test values. Fig 48 shows the ABAQUS moment distribution results and Fig 49 is the field test results.

The ABAQUS modelling gives good estimations of the peak bending moment in the pile beyond the excavation depth, however the estimation of bending moment in the embedded part is much higher, which may also caused by the higher soil stiffness in finite element modelling. Generally, the FE analysis of pit 2 gives reasonable results. Although the estimation of the behaviour of the embedded part of the pile is not accurate, the deflection of the pile beyond the excavation level will be more important, since the bending moment in the pile is much lower than the yielding point. There are some complexity in the field test that cannot be addressed in the FE modelling, however, the material

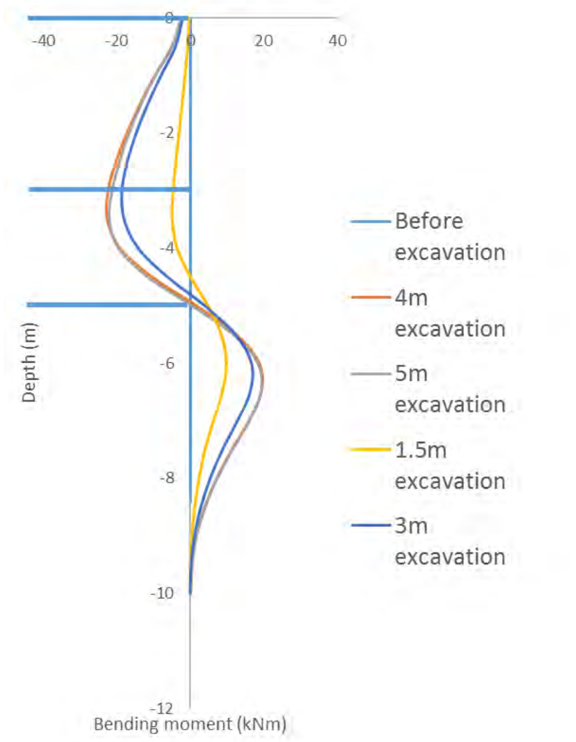

Figure 48: ABAQUS result

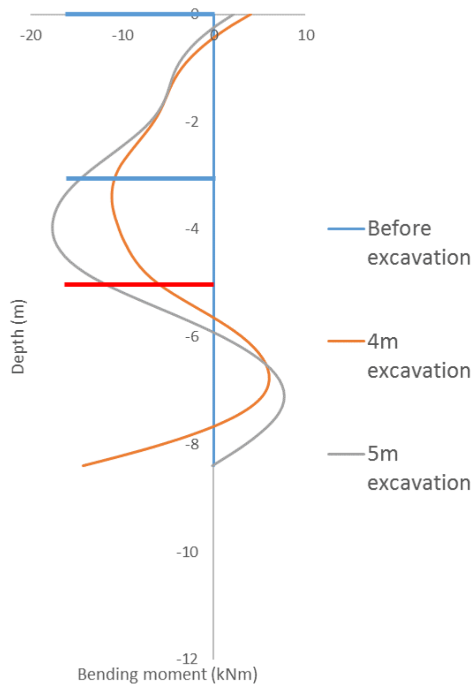

Figure 49: Pit2 field test bending moment

properties used here are still reasonable for the modelling of pit 1 in order to address the effectiveness of the bottom stabilisation.

4.5 Pit 1 modelling

4.5.1 Model with stabilisation process

Based on the material properties defined in previous section model of the first pit is created. The material properties to be used in this model are summarised in Tale 4 & 5.

Table 4: Soil properties

Friction angle	Unit weight	Cohesion	Voids ratio	Permeability
22°	20kN/m^3	6 kPa	0.7	0.0001 m^2

Table 5: Pile properties

E (Longitudinal)	E (Transvers)	Thickness	Poisson ratio	Shear modulus
210 GPa	10 GPa	8 cm	0.3	81 GPa

The stabilisation process is difficult to model, because we are not able to model the whole process of injecting concrete to form columns in the stabilisation zone. Based on the observation in previous sections, the stabilisation process will make the pile to deform because of injection of extra materials. The change in soil properties caused by the stabilisation process is hard to tell, but modelling this expansion effect is possible in ABAQUS CAE. Thermal expansion of the stabilisation zone is used to model the stabilisation process in this model. The steps of this numerical analysis are summarised below:

1. Initial step: Set initial temperature of all part to 273 K.
2. Step 1: Apply gravitational force to the whole model.
3. Step 2: Increase the temperature of the stabilisation zone in soil to simulate the stabilisation process.
4. Following steps: Simulate excavation and installation of props described in Section 3.3

The temperature increase in Step 2 is chosen by doing different trials to achieve similar deflection and bending moment magnitude as field test results near stabilisation zone. The final value of temperature increase used is 320 K.

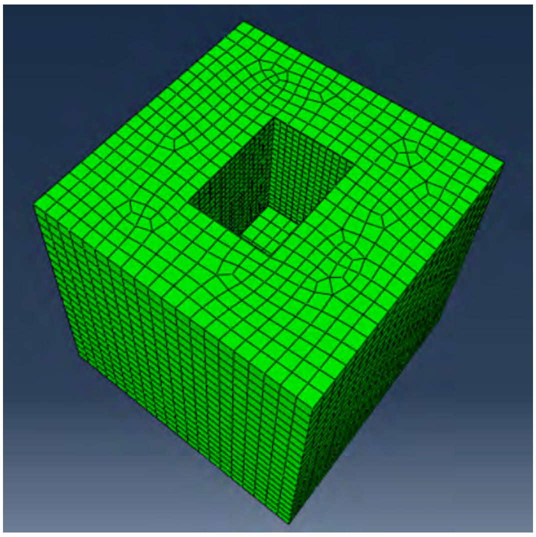

Figure 50: Pit 1 model

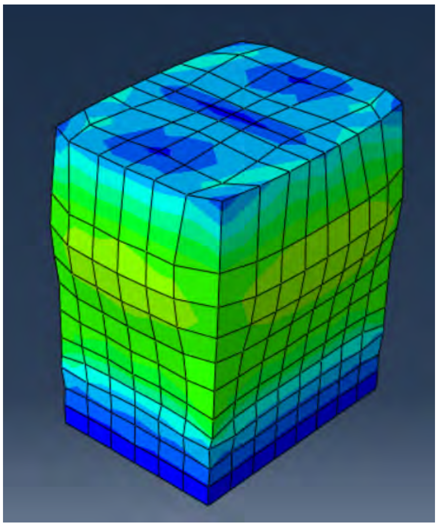

Figure 51: Soil expansion

Fig 51 shows the expansion of inner soil. Only top 3 m stabilisation zone is expanded, the expansion is restrained so that it only expand horizontally, because actual stabilisation process is done before excavation and soil still exist above the stabilisation zone, which will restrain the expansion vertically. The analysis was run and the results of deflection in different steps are plotted and compared with field test results.

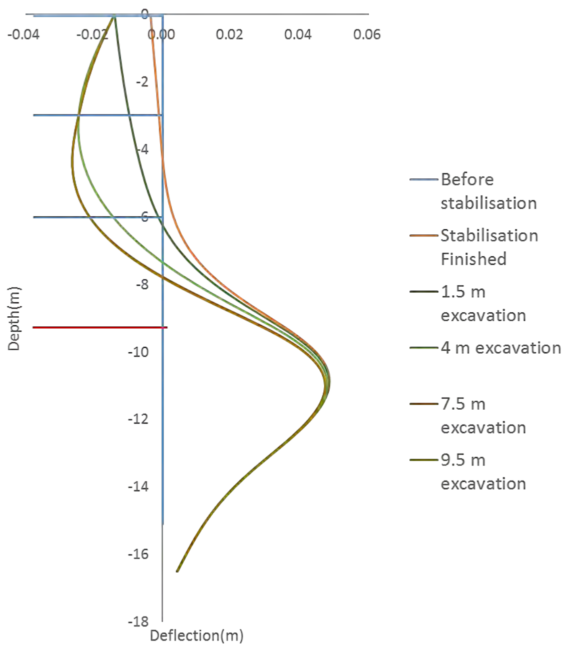

Figure 52: Deflection ABAQUS

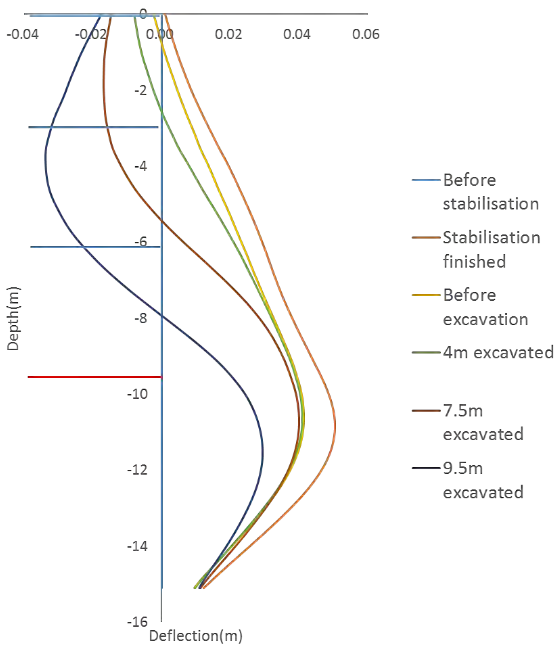

Figure 53: Deflection Field test

Fig 52 shows the ABAQUS analysis deflection of the pile and Fig 53 is the field test result. As discussed in Section 4.4.2, the gaps between props and wall during construction allows further deflection of the pile. From 7.5 to 9.5 m the ABAQUS model shows there is hardly any deflection will occur because of the third prop installed. Also same as pit 2 model, the embedded part of the pile doesn't deflect. Further analysis should be done by removing the prop effect to see whether the low deflection of embedded part is caused by the over design in the number of props. The FE analysis generally gives right prediction of deflection shape and deflection magnitude. The bending moment distribution are also compared. Fig 54 shows the ABAQUS modelling result and Fig 55 shows the field test result using inclinometer data. FE modelling gives good estimation of bending moment for embedded part of the beam, however the estimation for other part is not correct. The reason may still be the props, in Fig 54, the bending moment near the prop at -3 m becomes more positive after the installation of the prop. The gaps exist will alow the pile deflect more, so that the bending moment will keep increasing during the excavation process.

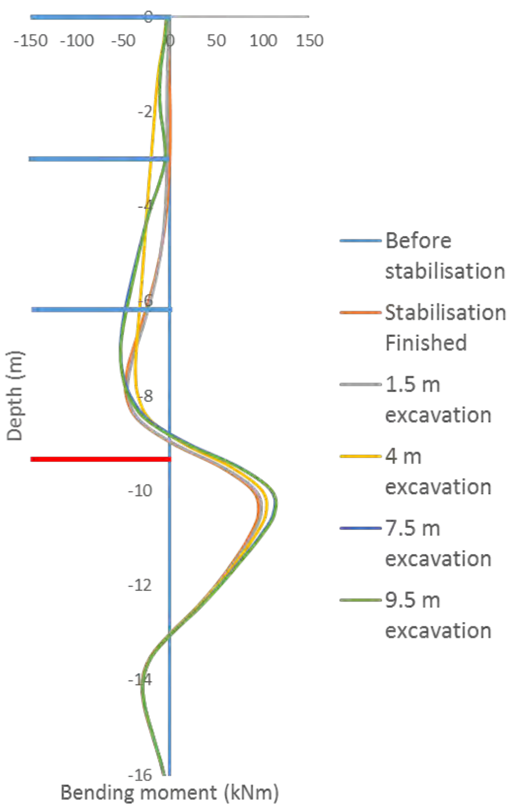

Figure 54: Bending moment ABAQUS

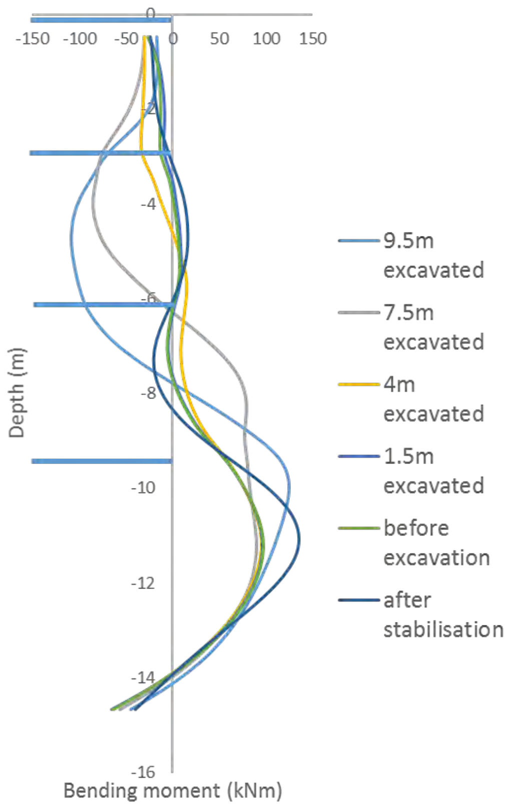

Figure 55: Bending moment Field test

4.5.2 Model without stabilisation process

The same model is used to analyse the behaviour of the pit without stabilisation process, by simply remove the soil expansion of stabilisation zone. The model is run and the results are compared with the previous model. Fig 56 shows the deflection shape of pit 1 without bottom stabilisation. The highest deflection is about 5 cm, which is 2 cm bigger than that with bottom stabilisation. However, because of the bottom stabilisation process the pile near the stabilisation zone will deflect about 5 cm. The results show that the stabilisation will effectively limit the deflection of pile above the excavation level. In this case by comparing the highest deflection of pile with and without bottom stabilisation a factor of safety of 1.5 can be achieved. For bending moment, no big difference can be observed, bottom stabilisation will generate big bending moment near the stabilisation zone, but the amount will not cause yielding or other structural failure of the pile.

As it was discussed before, since the bending moment in side the pile is much lower than the yield point of the pile, the deflection of the pile will be the only thing need to be limited. Traditional method is to add more props, which is time consuming and may cause congestion in the pit and difficult for excavator to operate. The stabilisation process gives more freedom in design. It can be used as part of the base slab to be used

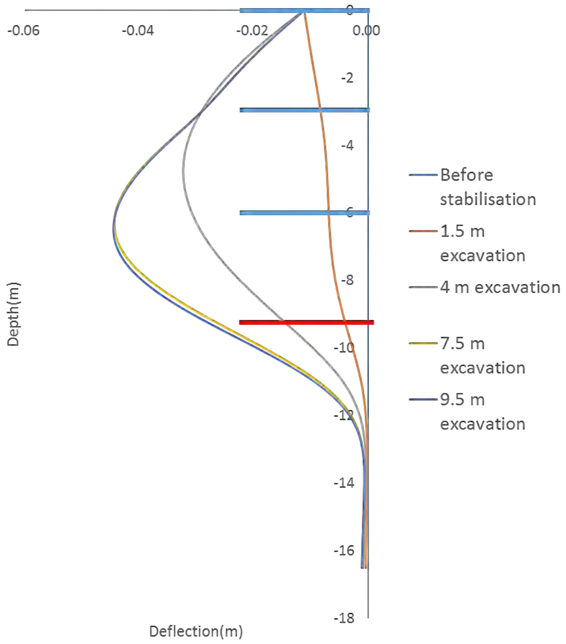

Figure 56: Deflection without stabilisation

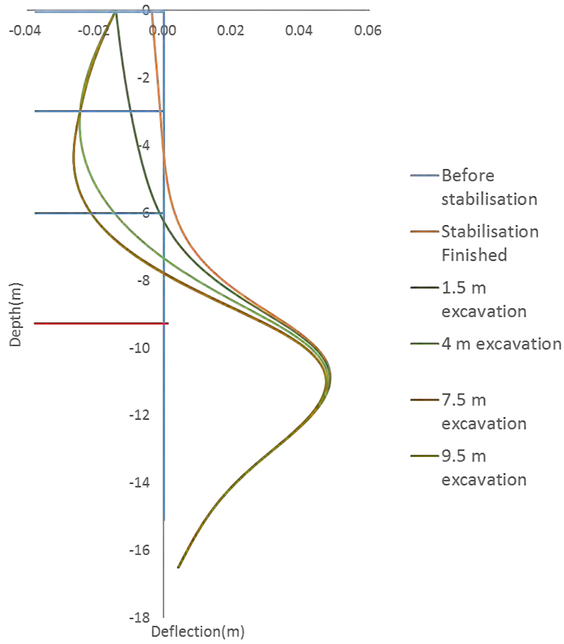

Figure 57: Deflection with stabilisation

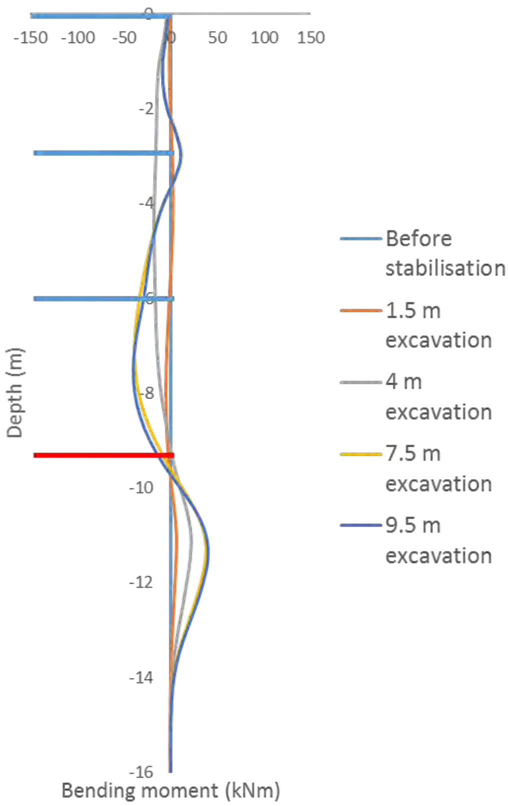

Figure 58: Bending moment without stabilisation

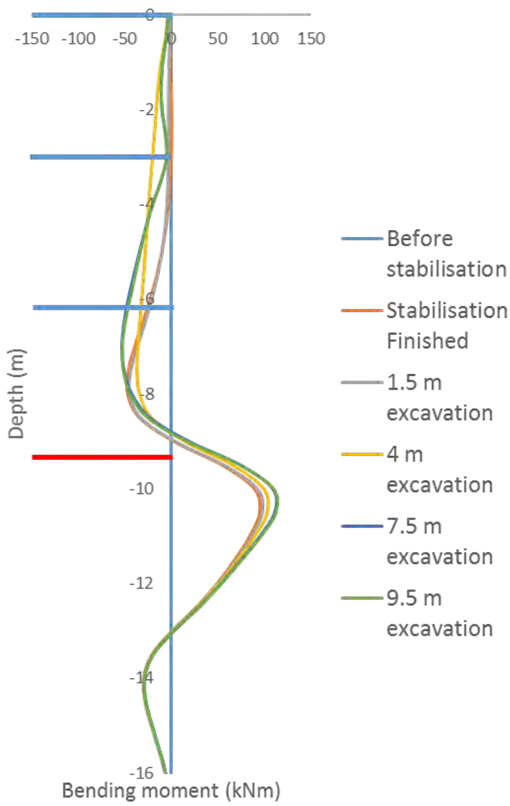

Figure 59: Deflection with stabilisation

during service of the underground space, the magnitude of deflection of pile that needs to be limited can be controlled by the amount of grouting injected.

4.6 Design of excel spreadsheets for retaining wall

From the deflection plot of pit 1 and pit 2 in numerical modelling analysis, points of fixity can be observed where during excavation the deflection is almost zero. The points are at about -11 m for pit 1 and about -7 m for pit 1. Based on this property design sheets based on superposition of cantilever behaviour can be created to obtain deflection or bending moment distribution of a retaining wall. The retaining structure can then be defined by the parameters shown in the Fig 60

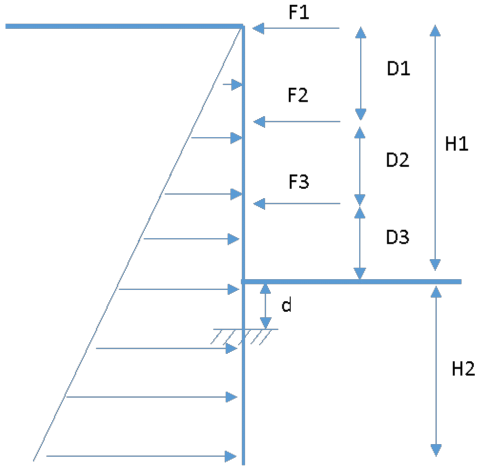

Figure 60: Simplified retaining structure

The numbers of props can be adjusted. The structural behaviour of the pile can be obtained by superposing the behaviour of several cantilever beam shown in Fig 61

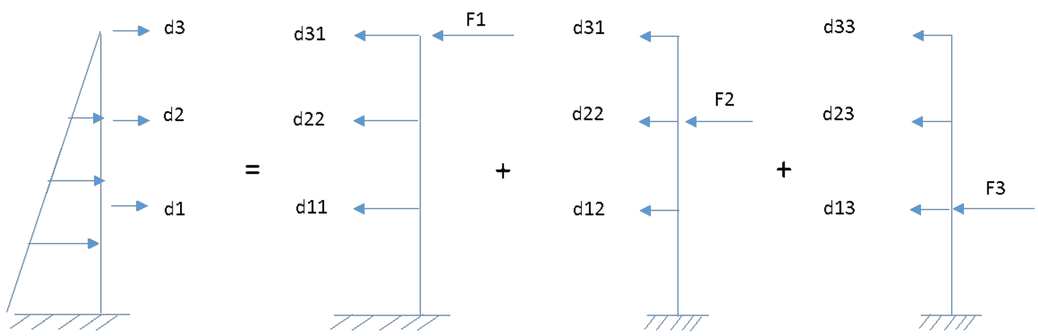

Figure 61: Superposition of cantilevers

The notation of d_{ij} means the deflection of the pile at the positions of the props in each load case. The deflections can be worked out based on beam databook. The prop forces can be then worked out using:

$$\begin{bmatrix} d_{11} & d_{12} & d_{13} \\ d_{21} & d_{22} & d_{23} \\ d_{31} & d_{32} & d_{33} \end{bmatrix} \begin{bmatrix} F1 \\ F2 \\ F3 \end{bmatrix} = \begin{bmatrix} d1 \\ d2 \\ d3 \end{bmatrix}$$

and

$$\begin{bmatrix} F1 \\ F2 \\ F3 \end{bmatrix} = \begin{bmatrix} d_{11} & d_{12} & d_{13} \\ d_{21} & d_{22} & d_{23} \\ d_{31} & d_{32} & d_{33} \end{bmatrix}^{-1} \begin{bmatrix} d1 \\ d2 \\ d3 \end{bmatrix}$$

When the forces are solved, the deflection and bending moment of the whole retaining wall can be solved. This approach ignore the passive soil pressure, and will be inaccurate if the point of fixity is much deeper. More experiments are also required to determine the position of the point of fixity.

4.7 Achievements and future work

The finite element modelling of the problem shows that the bottom stabilisation will decrease the deflection of the pile above the excavation level effectively. However, the relationship between amount of grouts and the effect of limiting deflection is still not clear. The amount of concrete used during field test is not accurately recorded, due to problems occur on site such as concrete stuck. More field tests on pits with different dimensions can be carried out in the future in order to address the problem. The suggested design spreadsheet is very preliminary and many assumptions are involved, but it is a starting point, future work of comparing this method with field test as well as numerical modelling may be useful.